Available online at www.sciencedirect.com
SCIENCE DIRECT®
ELSEVIER
Earth and Planetary Science Letters 211 (2003) 207–220
EPSL
www.elsevier.com/locate/epsl

Geochemical and Nd isotopic variations in sediments of the South China Sea: a response to Cenozoic tectonism in SE Asia☆

Xian-hua Li[a,*], Gangjian Wei[a], Lei Shao[b], Ying Liu[a], Xirong Liang[a], Zhimin Jian[b], Min Sun[c], Pinxian Wang[b]

[a] *Guangzhou Institute of Geochemistry, Chinese Academy of Sciences, P.O. Box 1131, Guangzhou 510640, PR China*
[b] *Laboratory of Marine Geology, Tongji University, Shanghai 200092, PR China*
[c] *Department of Earth Sciences, The University of Hong Kong, Pokfulam Road, Hong Kong, PR China*

Received 27 January 2003; received in revised form 16 April 2003; accepted 17 April 2003

Abstract

Secular variations in geochemistry and Nd isotopic data have been documented in sediment samples at ODP Site 1148 in the South China Sea. Major and trace elements show significant changes at ca. 29.5 Ma and 26–23 Ma, whereas ε_{Nd} values show a single change at ca. 26–23 Ma. Increases in Al/Ti, Al/K, Rb/Sr, and La/Lu ratios and a decrease in the Th/La ratio of the sediments beginning at 29.5 Ma are consistent with more intense chemical weathering in the source region. The abrupt change in Nd isotopes and geochemistry at ca. 26–23 Ma coincides with a major discontinuity in the sedimentology and physical properties of the sediments, implying a drastic change in sedimentary provenance and environment at the drill site. Comparison of the Nd isotopes of sediments from major rivers flowing into the South China Sea suggests that pre-27 Ma sediments were dominantly derived from a southwestern provenance (Indochina–Sunda Shelf and possibly northwestern Borneo), whereas post-23 Ma sediments were derived from a northern provenance (South China). This change in provenance from southwest to north was largely caused by ridge jumping during seafloor spreading of the South China Sea, associated with a southwestward expansion of the ocean basin crust and a global rise in sea level. Thus, the geochemical and Nd isotopic changes in the sediments at ODP Site 1148 are interpreted as a response to a major plate reorganization in SE Asia at ca. 25 Ma.

Keywords: South China Sea; geochemistry; Nd isotope; sediments; tectonism; weathering; Ocean Drilling Program

1. Introduction

The Cenozoic was a period of major tectonic activity in SE Asia and the SW Pacific, which had a significant impact on the landforms, climates, and life in the region [17]. The collision of India with Eurasia in the early Cenozoic closed the Tethyan ocean [1–3] and enlarged the land area

* Corresponding author. Tel.: +86-20-85290691; Fax: +86-20-85290130.
E-mail address: lixh@gig.ac.cn (X.-h. Li).

☆ Supplementary data associated with this article can be found at 10.1016/S0012-821X(03)00229-2

0012-821X/03/$ – see front matter
doi:10.1016/S0012-821X(03)00229-2

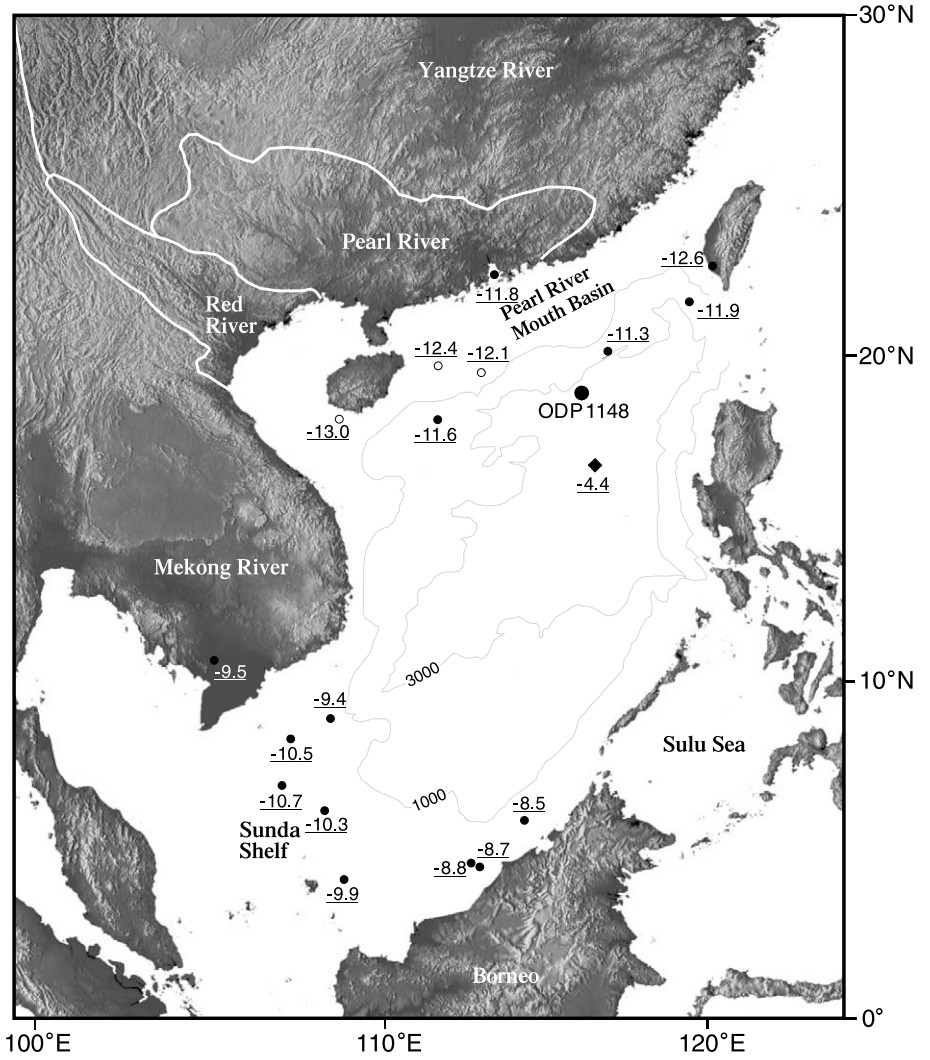

Fig. 1. Sketch bathymetric map of the SCS and surrounding regions showing sample locations including ODP Site 1148 (large solid dot), surface sediments from rivers and continental shelf and slope (small solid dots), sediments from petroleum exploration wells (small open circles) and a ferromanganese crust (solid diamond). The onshore relief is shown by a shaded topographic image with the extent of modern drainage of large rivers. Numbers near the sample locations are measured ε_{Nd} values.

of SE Asia. Continued convergence of India and Eurasia created the Tibetan Plateau by crustal shortening and thickening [4–7] and led to the southeastward crustal extrusion that caused the opening of the South China Sea (SCS) [8–11]. Uplift of the Tibetan Plateau most likely strengthened the Asian monsoon, thereby increasing the erosion rate and the flux of fluvial and eolian sediment into the Asian marginal seas [12–15].

In the middle to late Cenozoic, a series of major tectonic events occurred in SE Asia and the SW Pacific, such as the collision of New Guinea with the East Philippines–Halmahera–South Caroline Arc system, of Australia with SE Asia, of the Ontong Java Plateau with the Melanesian arc, and the arc–continent collision in Taiwan [16,17]. These events significantly changed the character of plate boundaries in much of SE Asia and influenced the development of landforms and life in the region.

Although tectonic activity and climate are clearly linked, the relationship between the two is complex and poorly understood. The marine sediments that fill the marginal seas of SE Asia were mostly derived from a number of large rivers that drain the Asian interior. Thus, these marine sediments should provide an ideal record of the erosional response to mountain building and climate change in Asia.

Sediments of the SCS were sampled during ODP Leg 184 in 1999. A continuous core 859.5 m long was recovered at ODP Site 1148 (18°50.17′N, 116°33.94′E), which is located on the distal passive margin of South China (Fig. 1). The oldest sediments at this site were deposited about 3 Myr prior to the onset of seafloor spreading in the SCS [18]. In order to explore the relationship between the tectonics, climate, and erosion in Asia since the opening of SCS, we conducted a systematic study of major and trace elements and Nd isotope compositions in the sediments recovered at ODP Site 1148.

2. Sedimentology of the drilled section

The sediments cored at ODP Site 1148 range in age from 32.8 Ma to the present [18]. The Lower Oligocene (32.8–28 Ma) section extends from the base of the hole at 860 mcd (meters composite depth) to 488 mcd, and consists predominantly of monotonous gray-green, quartz-rich nannofossil clay. Abundant opal-CT, which occurs in the sediment between 630 and 486 mcd [19], is of biogenic origin based on the presence of significant amounts of siliceous organic debris [20]. The Upper Oligocene section (28–23 Ma) contains a slump unit about 30 m thick between 458 and

Table 1
Biostratigraphic datum of planktonic foraminifera for sediments at ODP Site 1148

Code	Datum	Event	Depth (mcd)	Age (Ma)
PF		Pink *G. ruber*	16.11	0.12
PM		B/M boundary	57.36	0.78
PM		Top Jaramilo	71.26	0.99
PM		Base Jaramilo	75.16	1.07
PM		Top Olduvai	113.56	1.77
PM		Base Olduvai	120.66	1.95
PF	FO	*G. truncatulinoides*	124.42	2
PF	LO	*G. miocenica*	131.37	2.3
PF	LO	*G. altispira*	160.24	3.09
PF	LO	*S. seminulina*	162.54	3.12
PF		*Pulleniatina* (S–D)	174.04	3.95
PF	LO	*G. nepenthes*	175.90	4.2
PF	FO	*S. dehicene*	191.33	5.54
PF	FO	*G. tumida*	201.44	5.82
PF	LO	*G. mayeri*	277.56	10.49
PF	FO	*G. nepenthes*	287.11	11.19
PF	FO	*Orbulina*	316.53	15.1
PF	FO	*G. praescitula*	383.85	18.5
PF	LO	*P. kugleri*	417.53	21.5
PF	FO	*G. dehiscens*	456.51	23.2
PF	FO	*P. kugleri*	461.93	23.8
PF	FO	*P. pseudokugleri*	477.73	25.9
PF	LO	*P. opima opima*	482.53	27.1
PF	LO	*C. cubensis*	490.66	28.5
PF	FO	*G. angulosuturalis*	595.75	29.4
PF	LO	*Pseudohasterigerina* spp.	699.10	32
		Base	859.51	<33.7

PF = planktonic foraminifera; PM = paleo-magnetostratigraphy; FO = first occurrence; LO = last occurrence.

488 mcd. This unit, which consists mainly of nannofossil clay, was produced by mass flowage and slumping followed by gravitational redeposition. The Miocene and younger sections consist mainly of green-gray hemipelagic sediment with a decreasing content of biogenic carbonate upwards. A detailed description of the sedimentation at ODP Site 1148 is provided by Wang et al. [18].

3. Analytical methods

The sediment samples were leached with 1 M HCl to separate the residual fraction of aluminosilicates (containing undissolved opal, if present) from the biogenic/authigenic fraction of carbonate, organic matter and Fe–Mn oxyhydroxides [21]. The residual, aluminosilicate fractions were used for geochemical and Nd isotopic analysis. About 50 mg of sample was dissolved in screw-top Teflon beakers using a mixture of HF+HNO_3 for 7 days at 100°C. This technique typically results in complete digestion of clay samples. Any lack of digestion can be easily detected from the relative standard deviation (RSD) values of the analyzed elements. If the samples are not completely digested, for example, if minute zircon grains are present, the RSD values will be very high ($>10\%$) for Zr and Hf.

Major oxides (except SiO_2) and trace elements were determined using a Varian Vista PRO ICP-AES and a Perkin-Elmer Sciex ELAN 6000 ICP-MS, respectively, at the Guangzhou Institute of Geochemistry, Chinese Academy of Sciences. Cd and Rh internal standard solutions were used to monitor drift for the ICP-AES and ICP-MS analyses, respectively. The analytical precision is generally better than 1–2% for major elements and 1–3% for trace elements, including rare earth elements (REE) and refractory elements, such as Zr, Hf, Nb, and Ta. Relevant analytical details are described by Li et al. [22].

Nd samples were prepared by passing solutions through a cation column and then an HDEHP column. Nd isotopic compositions were determined using a Micromass Isoprobe multi-collector mass spectrometer (MC-ICPMS) at the Guangzhou Institute of Geochemistry. The MC-ICPMS was operated in static mode, and yielded $^{143}Nd/^{144}Nd = 0.512125 \pm 11$ (2σ) on 14 runs for the Shin Etsu JNdi-1 standard. Analytical procedures followed those of Liang et al. [23] modified after Vance and Thirlwall [24]. The $^{143}Nd/^{144}Nd$ ratios reported in this study are adjusted relative to the Shin Etsu JNdi-1 standard value of 0.512115 corresponding to the La Jolla standard value of 0.511858 [25]. A table of the geochemical and Nd isotopic data is presented in Appendix 1[1]. Age assignment for the sediments follows Wang et al. [18] and the revised biostratigraphic datum of planktonic foraminifera (Table 1). Some ages were interpolated between biostratigraphic data points using the average sedimentation rate.

4. Secular variation of geochemistry and Nd isotopes

Fig. 2 shows secular variations in the abundance of selected elements. All the elements, regardless of their geochemical behavior, show a remarkable jump in abundance at 477–455 mcd (ca. 26–23 Ma), with Ti, Rb, Zr, Nb, Ce, Sr, and Th increasing significantly by a factor of 2–7. Less pronounced shifts in concentration are shown for Ga, Ti, Rb, and Sr at ca. 600 mcd (ca. 29.5 Ma).

Fig. 3 shows the secular variation of several element ratios and Nd isotopes along with the mass accumulation rate (MAR). The Al/Ti, Al/K, Rb/Sr, La/Lu, and Th/La ratios display two remarkable shifts at ca. 600 mcd and 477–455 mcd. These two shifts generally coincide with two significant changes of the MAR.

Below 450 mcd (i.e., between 32.8 and 22.9 Ma) the MAR fluctuated significantly. During the period of rifting and seafloor spreading, MAR decreased rapidly from about 50 g/cm^2/kyr at the base of the section (ca. 32.8 Ma) to 6 g/cm^2/kyr at 630 mcd (30 Ma). During this time most elements and element ratios were roughly constant, or increased somewhat (Figs. 2 and 3). With the onset of seafloor spreading at 30 Ma, the MAR

[1] See the online version of this paper.

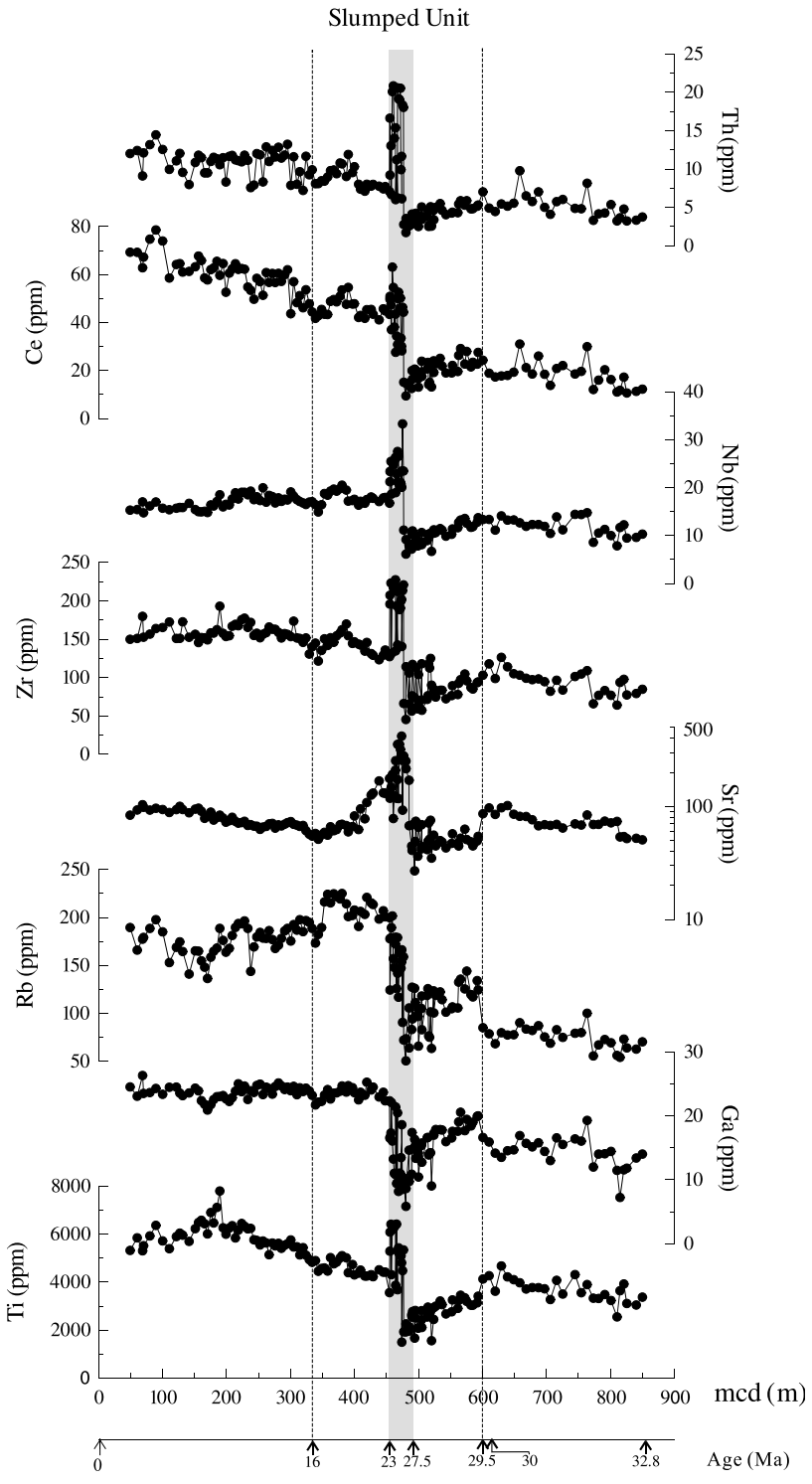

Fig. 2. Secular variations of abundance for selected elements.

increased from 6 g/cm^2/kyr at 630 mcd to about 20 g/cm^2/kyr at 589 mcd, whereas most element ratios increased abruptly at 600 mcd (ca. 29.5 Ma). The MAR remained high and constant (about 20 g/cm^2/kyr) between 589 and 497 mcd (29.3–28.5 Ma), and then decreased again to 0 g/cm^2/kyr at 477 mcd (ca. 26 Ma). This quick decrease in the MAR coincides with development of the slump unit and with marked changes in sedimentology, physical properties, geochemistry, and Nd isotopes of the sediments.

The abrupt change in geochemistry takes place mostly between 477 mcd (ca. 26 Ma) and 455 mcd (ca. 23 Ma). For example, the Al/K, Th/Cr, Th/La, La/Lu, and Al/Ti ratios change markedly across an interval of high variability between 477 and 455 mcd (ca. 26–23 Ma) (Fig. 3). The zone of high variability slightly postdates the development of the slump unit at 488 mcd (ca. 28 Ma) and the sharp decrease in MAR at 497 mcd (28.5 Ma), but coincides exactly with the lowest MAR at 477 mcd. In contrast, the ε_{Nd} values fluctuate significantly but show only a steady decrease from −10 at 480 mcd to −13 at 460 mcd.

5. Geochemical response to increased weathering at ca. 30 Ma

The geochemistry of clastic sediments is controlled by numerous factors, such as provenance composition, chemical weathering, hydraulic sorting, diagenesis, and alteration [26]. Alkali and alkaline earth elements, which are concentrated in rock-forming minerals, such as Rb and K in K-feldspar and biotite and Sr in plagioclase, are chemically mobile in sedimentary environments [27]. Thus, the Rb/Sr and Al/K ratios of lithogenic residual fractions are good indicators of the degree of weathering. In contrast, high-field-strength (HFS) elements, such as Ti, Zr, and Nb, which are concentrated mainly in accessory heavy minerals, are chemically immobile.

A recent study of element mobility during weathering of granodiorite by Nesbitt and Markovics [28] showed that both Th and Al are mobilized during chemical weathering. Weathered samples in this study all had Al/Ti and Th/Ti ratios about 50% and 100% higher, respectively, than the fresh parent granodiorites. On the other hand, all weathered samples, regardless of their degree of weathering, had similar Al/Ti and Th/Ti ratios. REE appear more mobile than Th, but have a relatively complicated behavior. Weakly to moderately weathered samples are significantly enriched, twofold to threefold, in total REE content but have nearly identical La/Lu ratios as the parent rock. Strongly weathered soil displays somewhat lower total REE contents, but significantly higher La/Lu ratios, than the parent rock. The weathered soils generally have lower Th/La ratios than the parent rock, because Th is less enriched than La during weathering. Some workers believe that the chemically immobile HFS element ratios of clastic sediments can be used as tracers of the sedimentary sources [26], but these HFS elements can be affected by non-chemical processes such as hydraulic sorting. In general, it is difficult to deduce the sedimentary provenance simply from the geochemistry of sediments. On the other hand, the Nd isotopic composition of sediments is considered an ideal tracer of sedimentary provenance [29] because it is a fingerprint of the source materials, unaffected by either weathering or sedimentary processes.

The first geochemical discontinuity in the sediments at ODP Site 1148, at about 600 mcd, shows a significant increase in most element ratios, particularly Al/Ti, Rb/Sr, La/Lu, and Al/K (Fig. 3). These ratios increase by a factor of about 1.5–3 whereas the Th/La ratio decreases by a factor of 2 (Fig. 3). Unlike element concentrations that could be diluted by opal in the residual fractions, these element ratios would be unaffected. The changes in element ratios at about 600 mcd, combined with insignificant changes of HFS element abundances, most likely reflect an important change in the nature or degree of chemical weathering in the source regions at ca. 29.5 Ma. A significant provenance change at about 600 mcd is unlikely because there is no significant change in the Nd isotopic composition across this discontinuity.

Significant increases in Al/K and Rb/Sr ratios, which are measures of chemical weathering, between 600 and 477 mcd suggest more intense

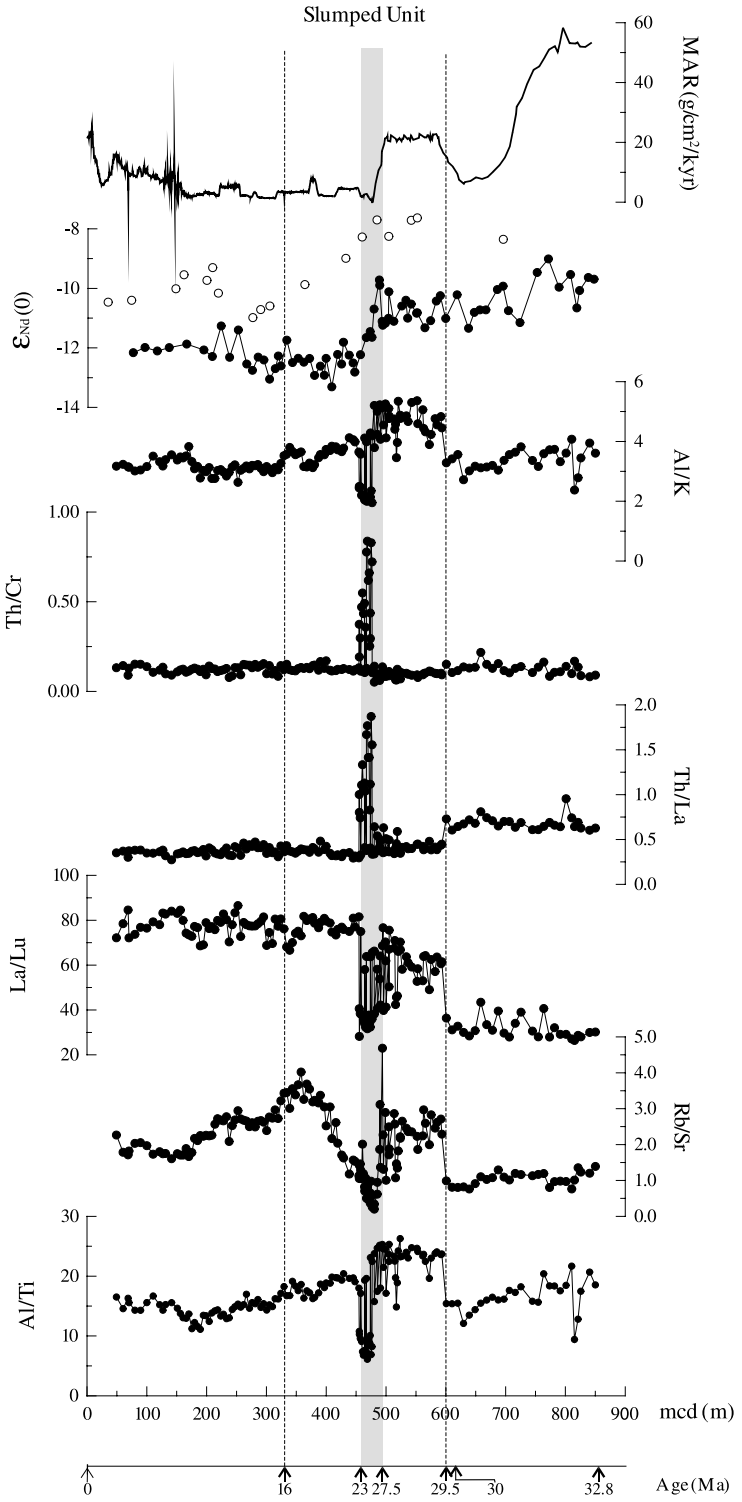

Fig. 3. Secular variations of selected element ratios and Nd values as well as the mass accumulation rate (MAR) [18]. The ε_{Nd} values of Clift et al. [19] are plotted as open circles for comparison.

chemical weathering in the source region [27]. The increase of Al/Ti and decrease of Th/La ratios between 600 and 477 mcd also suggest more intense weathering, as does the two-fold increase in the La/Lu ratio at 600 mcd. There is no significant change in REE abundance at 600 mcd, but there is a slight decrease in REE abundance (such as Ce, Fig. 2) between 600 and 477 mcd.

The more intense weathering inferred at 29.5 Ma roughly coincides with the initiation of seafloor spreading in the SCS at Chron 11 (30 Ma) [10,30] as shown by the sharp change of MAR at about 630 mcd (Fig. 3). The relationship, if any, between these two events is unknown.

Although many researchers have proposed that rapid uplift of the Tibetan Plateau at ca. 10–8 Ma [12,31,32], or more recently [33], or in multiple stages [15] strengthened the monsoon and changed the climate of Asia, the geological effects of this change are unclear. An alternative hypothesis, proposed by Ramstein et al. [34], is that monsoon development coincided with the closure of Paratethys in central Asia at ca. 30 Ma, i.e., much earlier than uplift of the Tibet Plateau. All we can say at the present time is that the geochemical changes observed in the SCS at 29.5 Ma support an increase in the intensity of chemical weathering in the source region.

6. Nd isotopic response to the provenance change from the south to the north at ca. 26–23 Ma

The most pronounced geochemical change in the SCS sediments is recorded between 477 and 455 mcd (ca. 26–23 Ma). In addition to marked changes in element concentrations and element ratios, there is an abrupt decrease in ε_{Nd} from −10 to −13 (Fig. 3). This geochemical and Nd isotopic change corresponds closely to significant changes in the physical properties of the sediments, particularly color reflectance, natural γ-radiation, magnetic susceptibility, porosity, and density [18]. This major discontinuity corresponds approximately to the 'slumped unit' and the 'Late Oligocene unconformity' at Site 1148 [18], although the 'slumped unit' occurred ca. 2 Ma earlier than the geochemical and Nd isotopic shifts. This discontinuity clearly marks a major geologic event at ca. 26–23 Ma, which significantly changed both the sedimentary environment at ODP Site 1148 and the provenance of the sediments.

Clift et al. [19] recently reported preliminary Nd isotopic analyses for the <2 μm clay fraction of 18 samples at Site 1148. Their results show a similar temporal variation pattern to that reported here. They compared the Nd isotopic composition of sediments with that of possible source rocks in continental Asia and concluded that South China was the major sediment source.

However, there are some differences in the Nd isotopic results reported by Clift et al. [19] and those presented here. First, due to lower-resolution analyses, their data show a gradual, rather than abrupt change at ca. 470 mcd. More importantly, the $^{143}Nd/^{144}Nd$ ratios reported by Clift et al. [19] are about 0.02–0.03% (2–3 ε_{Nd} units) higher than ours for given samples or given depths. These differences most likely reflect analysis of different sediment size fractions. Clift et al. [19] analyzed only the clay fraction (<2 μm) whereas we analyzed the bulk aluminosilicate fraction. Marine sediments contain both detrital and authigenic clay minerals and the latter have Nd isotopic compositions that equilibrated with seawater [35]. As an example, we analyzed a ferromanganese crust from the central SCS and obtained a $^{143}Nd/^{144}Nd$ ratio of 0.512410 ± 7, indicative of the Nd isotopic composition of modern SCS seawater. This value is comparable with the modern Pacific Ocean seawater values of 0.5124–0.5126 [36], but significantly higher than those of the residual, aluminosilicate fraction of sediments at ODP Site 1148. Thus, the Nd isotopic difference of about 0.02–0.03% (2–3 ε_{Nd} units) between clay fraction [19] and bulk aluminosilicate fraction (this study) is mostly attributed to the relative proportion of authigenic clay in the analyzed fractions. Our grain size analysis indicates that the <2 μm clay fraction is about 10–20% in the sediments at Site 1148. Thus, the authigenic clay with a seawater $^{143}Nd/^{144}Nd$ ratio of 0.51241 constitutes a much higher proportion (30–60%) of the clay size fraction than of the bulk aluminosilicate fraction (<5–10%). Appar-

ently, the bulk aluminosilicate fraction yields $^{143}Nd/^{144}Nd$ ratios slightly higher (<0.5–1 ε_{Nd} unit) than the average Nd isotopic composition of the sediment source material provenance, whereas the bulk clay fraction has a composition at least 2–3 ε_{Nd} units higher than that of the source.

Proper estimation of the Nd isotopic variation of possible sources is fundamental for Nd isotopic provenance analysis. For a given source terrane, such as South China, the exposed rock types have a wide range of Nd isotopic compositions [37], with Nd model ages (T_{DM}) ranging from Archean to Neoproterozoic corresponding to the present-day ε_{Nd} values of about 0 to −25. Rock types exposed within the modern Pearl River drainage (Fig. 1) include Proterozoic to Cenozoic igneous and sedimentary rocks, which also have a wide range of Nd isotopic compositions. This wide range of values contrasts significantly with the assigned narrow range of −9 to −11 for South China [19]. An alternative approach of estimating the average Nd isotopic composition of a source terrane is to analyze particulates and sediment from major rivers that drain an 'average' exposed continental crust [36,38]. In this study, we analyzed Nd isotopic ratios for sediments supplied to the SCS, including those from the Gau-Pin River in southwestern Taiwan, the Pearl River, the Pearl River Mouth basin, the South China

Table 2
Nd isotopes for sediments around SCS and a ferromanganese crust from central SCS

Sample	Location	Age	$^{143}Nd/^{144}Nd$	ε_{Nd}
Gau-Pin River (SW Taiwan)				
E213	22°53.8′N, 120°28.7′E	Quaternary	0.512006 ± 10	−12.3
E230	22°53.8′N, 120°28.7′E	Quaternary	0.511989 ± 9	−12.7
E242	22°53.8′N, 120°28.7′E	Quaternary	0.511985 ± 6	−12.7
NE South China Sea				
79-38	21°32.00′N, 119°48.00′E	Modern-day	0.512029 ± 8	−11.9
Pearl River Mouth				
LDY-1	22°14.4′N, 113°35.4′E	Modern-day	0.512037 ± 9	−11.7
LDY-2	22°14.4′N, 113°35.4′E	Modern-day	0.512033 ± 6	−11.8
LDY-3	22°14.4′N, 113°35.4′E	Modern-day	0.512029 ± 7	−11.9
Pearl River Mouth basin				
ODP1144A05H01W45-50	20°03.18′N, 117°25.14′E	Quaternary	0.512049 ± 7	−11.5
ODP1144A09H01W45-50	20°03.18′N, 117°25.14′E	Quaternary	0.512055 ± 7	−11.4
ODP1144A15H01W45-50	20°03.18′N, 117°25.14′E	Quaternary	0.512067 ± 8	−11.1
LH19-4-1/1685	Zhu3 depression	Miocene	0.512021 ± 8	−12.0
LH19-4-1/1706	Zhu3 depression	Miocene	0.512006 ± 8	−12.3
LH19-4-1/1760	Zhu3 depression	Miocene	0.512027 ± 9	−11.9
PY33-1-1/3450	Zhu3 depression	Oligocene	0.512003 ± 8	−12.4
NW South China Sea				
83-18	18°0.03′N, 111°59.13′E	Modern-day	0.512043 ± 7	−11.6
13-1-8/2987	Qiongdongnan Basin	Pliocene	0.511972 ± 9	−13.0
Offshore Indochina				
NS90-68	8°22.27′N, 107°22.97′E	Modern-day	0.512102 ± 9	−10.5
NS90-70	8°52.02′N, 108°39.90′E	Modern-day	0.512155 ± 7	−9.4
Sunda Shelf				
NS90-54	6°51.22′N, 107°09.57′E	Modern-day	0.512088 ± 8	−10.7
NS90-40	6°08.16′N, 108°37.67′E	Modern-day	0.512111 ± 7	−10.3
Offshore Borneo				
NS89-61	4°04.35′N, 109°03.97′E	Modern-day	0.512129 ± 8	−9.9
NS88-62	4°33.96′N, 113°5.84′E	Modern-day	0.512189 ± 7	−8.8
NS88-68	4°24.22′N, 113°20.17′E	Modern-day	0.512191 ± 7	−8.7
NS88-44	5°49.07′N, 114°39.07′E	Modern-day	0.512200 ± 8	−8.5
Ferromanganese crust				
Xian-1	16°40′N, 116°50′E	Modern-day	0.512410 ± 7	−4.4

continental slope (ODP Site 1144), northeastern and northwestern SCS, the Sunda Shelf and offshore SE Indochina and northern Borneo (Table 2). The results, together with Nd isotopic data for river particulates from the Mekong River [36], are plotted in Fig. 1 and compared with the Nd isotopic data for sediments at ODP Site 1148 in Fig. 4. The sediments north of the SCS have a restricted range of ε_{Nd} values (−11 to −13), comparable with the Nd isotopic compositions of Cenozoic sediments in Taiwan that were derived from South China [39]. These results indicate that the sediments derived from the South China terrane had fairly constant ε_{Nd} values (−11 to −13) during the Cenozoic. These values yield an average crustal residence age of 1.7–1.9 Gyr for the northern (South China) provenance, which is similar to the majority of T_{DM} ages for the crustal rock in the Cathaysian Interior of South China [37]. In contrast, sediments from the Mekong River and offshore Indochina, Sundaland and Borneo to the south and southwest of the SCS have clearly higher ε_{Nd} values of −8.5 to −11, corresponding to an average crustal residence age of 1.5–1.7 Gyr for this southern provenance. Sm–Nd isotopic data are quite limited in the literature for this vast area. The metasedimentary rocks and granites in peninsular Malaysia exhibit T_{DM} ages that cluster around 1.5–1.8 and 1.1–1.5 Gyr, respectively [40]. The Dienbien granitoid complex in northern Vietnam (south of the Song Ma suture zone) yields T_{DM} ages of 1.4–1.5 Gyr [41]. These limited Nd isotopic data indicate that the most important crustal formation of Indochina–Sundaland probably took place in the Mesoproterozoic, a few hundreds of million years later than in South China. Although Sm–Nd isotopic data are not available for Borneo, geochemical data indicate that the Tertiary magmatic belt in northern Borneo is composed of calc-alkaline volcanic rocks related to subduction of the proto-SCS [42]. These subduction-related basaltic to felsic volcanic rocks should have higher ε_{Nd} values than the surrounding crustal basement due to the involvement of various amounts of mantle material in their formation. Among the analyzed sediments surrounding the SCS, those from offshore Borneo have the highest ε_{Nd} values (−8.5 to −8.8), indicating a possible contribution from these volcanic rocks.

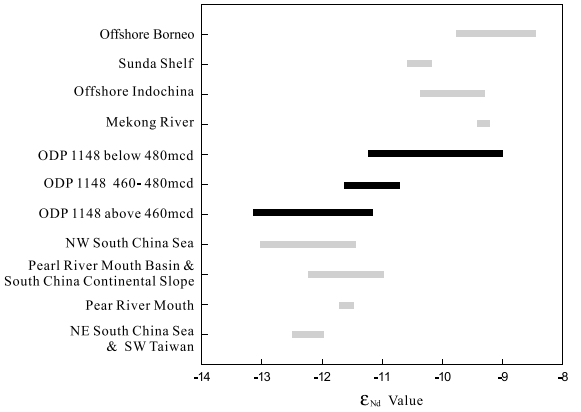

Fig. 4. Comparison of the Nd values of sediments at ODP Site 1148 with possible sources surrounding the SCS. Data from the particulates of Mekong River are after Goldstein et al. [36].

Pre-27 Ma and post-23 Ma sediments at ODP Site 1148 exhibit ε_{Nd} values comparable, respectively, with those of the northern (South China) and southern (Indochina–Sundaland–Borneo) sources (Fig. 4). Thus, a rapid change of sediment provenance predominantly from a southern drainage to a northern drainage might have occurred during the 26–23 Ma interval.

Clift et al. [19] proposed that the relatively high ε_{Nd} values in sediments below 480 mcd could be explained by significant addition of volcanic material into the sediments following rifting and seafloor spreading in the SCS. We do not believe that the sediment geochemistry, e.g. the Th/Cr ratios (Fig. 3), supports this interpretation. All of the sediments at ODP Site 1148 except those between 477 and 455 mcd have low Th/Cr ratios of 0.1–0.2, characteristic of material derived from continental crustal material [43]. However, the sediments in the interval 477–455 mcd have significantly higher Th/Cr ratios (up to 0.8), typical of intermediate to silicic igneous debris. This enrichment in Th is associated with increases in Ti, Nb, Zr, Sr, and REE and decreases in Rb and Ga. Thus, the composition of the sediments in the 477–455 mcd interval most likely reflects a major contribution of intermediate to silicic igneous material (with enriched accessory mineral fractions?)

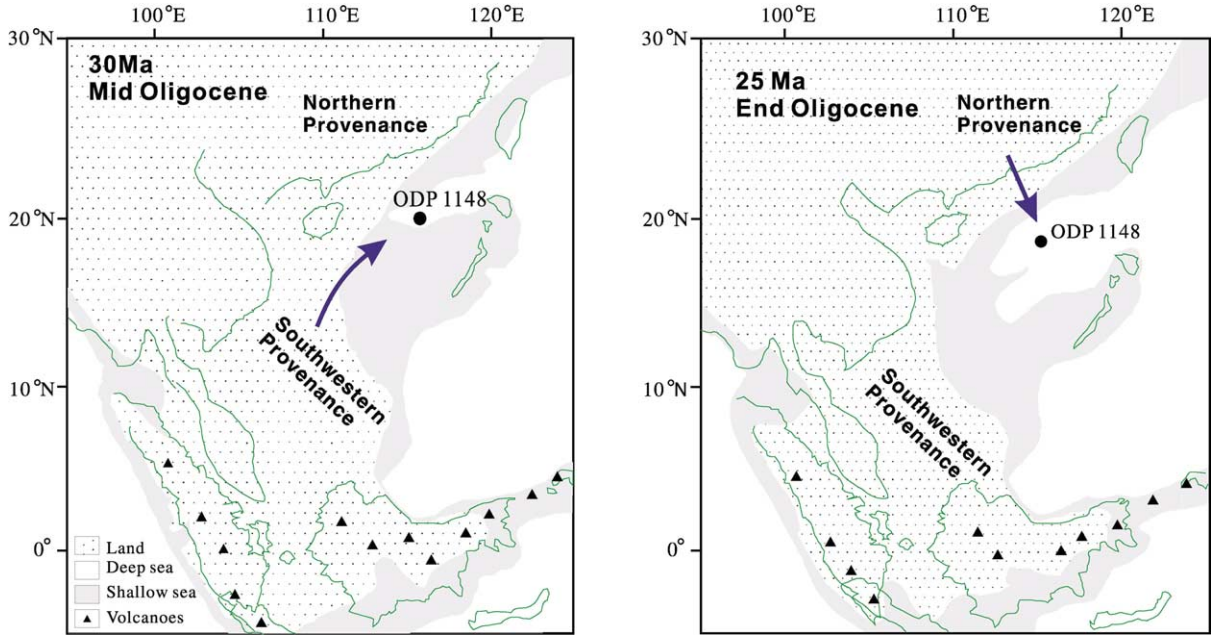

Fig. 5. Distribution of land and sea in SE Asia at 30 Ma (left) and 25 Ma (right), modified after Hall [16]. The vast areas of Sundaland and the Sunda Shelf were exposed during the middle Oligocene and transportation of sediments from the vast, emergent land to ODP Site 1148 was possible. The area of the emergent Sundaland and Sunda Shelf decreased along with the global sea level rise at the end of the Oligocene. At the same time, the oceanic spreading of SCS propagated southwestwards, resulting in an enlarged, V-shaped area of oceanic crust.

to the sediment provenance at ca. 26–23 Ma, whereas the remainder of the sediments was probably derived from a continental source.

7. Tectonic implications

Considering the present-day geographical location of ODP Site 1148 east of Hainan Island, the Pearl River is most likely the principal source of clastic material currently being deposited on the outer continental slope. The rapidly uplifting, young mountains of Taiwan may also contribute some material [44], whereas the Red River is mostly shielded from the site by Hainan Island. Our Nd isotopic data suggest that South China has been the main source of sediments since 23 Ma, but that a different provenance existed before 26 Ma.

The geological evolution of the Pearl River Mouth basin can be divided into two stages separated by a breakup unconformity near the Early/Late Oligocene boundary: (1) basement rifting, forming a series of alternating rises and depressions filled by tilted and disturbed non-marine clastic rocks of Upper Cretaceous to Early Oligocene age, and (2) subsidence and filling of the entire basin with predominantly marine sediments since the Late Oligocene [45,46]. The detritus carried by the Pearl River (or its precursor) was mostly trapped within these depressions, and separated from the outer shelf by a series of rises before the Late Oligocene. Thus, the majority of the detritus from South China was probably not transported as far as ODP Site 1148 until the depressions were filled in and coalesced to form a single basin during nannofossil Zone NP24 [46].

Transportation of clastic sediments from Borneo to ODP Site 1148 seems unlikely because the two areas have been separated by the SCS since 30 Ma and by the proto-SCS prior to 30 Ma. Transportation of clastic sediments from southwestern sources (Indochina, Sundaland and possibly part of northwestern Borneo) to ODP Site

1148 would also have been difficult because of separation by the southwestern SCS since it opened between Chron 7 and C6b ca. 25–23 Ma [10,30] (Fig. 5). However, such transportation could possibly have occurred prior to 26 Ma.

According to Haq et al. [47], the middle Oligocene between 33 and 28.5 Ma was a time of much lower sea level. Thus, vast areas of Sundaland and the Sunda Shelf were exposed (Fig. 5), and transportation of sediments from this emergent landmass to ODP Site 1148 was clearly possible before and shortly after opening of the SCS. Appearance of abundant opal-CT formed from radiolarians, diatoms, and sponge spicules between 630 and 486 mcd suggests a high productivity of biogenic silica shortly after the opening of the SCS at 30–28 Ma [20]. A high productivity of biogenic silica suggests that ODP Site 1148 was, at that time, a near-shore environment where nutrient supply was high. This is in contrast to the large ocean basin of the present-day SCS, far away from the continent, where biogenic productivity is very low [48].

Based on the geochemical and isotopic character of the sediments at ODP Site 1148, a major change in provenance occurred at 26–23 Ma. A major plate reorganization took place in SE Asia at ca. 25 Ma [16,17], probably caused by a series of tectonic collisions, e.g., the collision of New Guinea with the East Philippines–Halmahera–South Caroline Arc system, the collision of the Ontong Java Plateau with the Melanesian Arc, and the collision of the Australian continent with SE Asia. Major changes in the SCS and surrounding continents correlate closely with this major plate reorganization. For example, the southern segment of the Ailao Shan–Red River (ASRR) shear zone was uplifted and cooled rapidly in the Early Miocene (25–22 Ma) [49–51] and leucogranites were emplaced in and near the ASRR shear zone between 27 and 22 Ma [52–54]. Movement on the ASRR shear zone changed from transpressional to transtensional at 28–24 Ma [55] and the Wang Chao and Three Pagodas fault systems developed dextral movement at ca. 23 Ma [56]. All these changes are believed to be related to intensified extrusion of Indochina along the ASRR fault in Oligo–Miocene time.

In the SCS, the spreading ridge jumped from the north to the southwest at Chron 7 to C6b at 25–23 Ma [10,30]. Propagation of spreading southwestwards resulted in an enlarged, V-shaped area of oceanic crust (Fig. 5). Meanwhile, the ocean area expanded rapidly as the global sea level rose at 28.5–24 Ma [47], and the emergent portions of Sundaland and the Sunda Shelf decreased significantly during this period (Fig. 5). This would have greatly reduced the transport of sediment from a southwestern source.

8. Conclusions

Geochemical and Nd isotopic analysis for sediments at ODP Site 1148 reveals two significant changes of major and trace elements at ca. 29.5 Ma and 26–23 Ma and a single change of ε_{Nd} values at 26–23 Ma. Increases in Al/Ti, Al/K, Rb/Sr, and La/Lu ratios and a decrease in the Th/La ratio of the sediments beginning at 29.5 Ma suggest an increase in the intensity of chemical weathering in the source region. The abrupt change in Nd isotopes at ca. 26–23 Ma, along with a major discontinuity in the geochemistry, sedimentology, and physical properties of the sediments, implies a drastic change in sedimentary provenance and environment at the drill site. Nd isotopic analyses of sediments from major rivers flowing into the SCS indicate two major provenances, i.e. a northern provenance of South China and a southwestern to southern provenance of Indochina–Sunda Shelf and Borneo. Pre-27 Ma sediments were dominantly derived from the southwestern provenance, whereas post-23 Ma sediments were derived from the northern provenance. This provenance change of the sediments at ca. 26–23 Ma appears to have been largely caused by a ridge jump from the north to the southwest, associated with a southwestward expansion of the ocean basin and a rise in sea level.

Acknowledgements

We thank T. Lee, A. Yin, S.S. Sun, Z.X. Li, S.-L. Chung and J.X. Zhao for helpful discussions

and P. Robinson for proofreading the paper. The sediment samples were provided by the Ocean Drilling Program and the South China Sea Institute of Oceanology, Chinese Academy of Sciences. Reviews and constructive comments by Steven L. Goldstein, Robert Hall and S.-L. Chung substantially improved the manuscript. This work was supported by the National Natural Science Foundation of China (Grant 49999560) and the Chinese Academy of Sciences (Grant KZCX2-102).*[RV]*

References

[1] D.B. Rowley, Age of initiation of collision between India and Asia: a review of stratigraphic data, Earth Planet. Sci. Lett. 145 (1996) 1–13.
[2] Y. Najman, E. Garzanti, Reconstructing early Himalayan tectonic evolution and paleogeography from Tertiary foreland basin sedimentary rocks, northern India, Geol. Soc. Am. Bull. 112 (2000) 435–449.
[3] C. Wang, X. Li, X. Hu, L.F. Jansa, Latest marine horizon north of Qomolangma (Mt Everest): implications for closure of Tethys seaway and collision tectonics, Terra Nova 14 (2002) 114–120.
[4] P. England, G. Houseman, Finite calculation of continental deformation 2. Comparison with the India–Asia collision zone, J. Geophys. Res. 91 (1986) 3664–3676.
[5] J.F. Dewey, S. Cande, W.C. Pitman, Tectonic evolution of the India/Eurasia collision zone, Eclogae Geol. Helv. 82 (1989) 717–734.
[6] G. Houseman, P. England, Crustal thickening versus lateral expulsion in the Indian–Asian continental collision, J. Geophys. Res. 98 (1993) 12233–12249.
[7] G. Houseman, P. England, A lithospheric-thickening model for the Indo-Asian collision, in: A. Yin, M. Harrison (Eds.), The Tectonic Evolution of Asia, Cambridge University Press, New York, 1996, pp. 1–17.
[8] P. Tapponnier, G. Peltzer, R. Armijo, A.-Y. Le Dain, P. Cobbold, Propagating extrusion tectonics in Asia: New insights from simple experiments with plasticine, Geology 10 (1982) 611–616.
[9] P. Tapponnier, G. Peltzer, R. Armijo, On the mechanics of the collision between India and Asia, in: M.P. Coward, A.C. Pies (Eds.), Collision Tectonics, Geol. Soc. London Spec. Publ. 19 (1986) 115–157.
[10] A. Brias, P. Patriat, P. Tapponnier, Updated interpretation of magnetic anomalies and seafloor spreading stages in the South China Sea: Implications for the Tertiary tectonics of Southeast Asia, J. Geophys. Res. 98 (1993) 6299–6328.
[11] P.H. Leloup, N. Arnaud, R. Lacassin, J.R. Kienast, T.M. Harrison, T.T. Phan, T.A. Replumaz, P.J. Tapponnier, New constraints on the structure, thermochronology and timing of the Ailao Shan-Red River shear zone, SE Asia, J. Geophys. Res. 106 (2001) 6683–6732.
[12] P. Molnar, P. England, J. Martiod, Mantle dynamics, uplift of the Tibetan Plateau and the Indian monsoon development, Rev. Geophys. 34 (1993) 357–396.
[13] J.E. Kutzbach, W.L. Prell, W.F. Ruddiman, Sensitivity of Eurasian climate to surface uplift of the Tibetan Plateau, J. Geol. 101 (1993) 177–190.
[14] D.K. Rea, H. Snoeck, L.H. Joseph, Late Cenozoic eolian deposition in the North Pacific: Asian drying, Tibetan uplift, and cooling of the Northern Hemisphere, Paleoceanography 13 (1998) 215–224.
[15] Z. An, E.J. Kutzbach, W.L. Prell, S.C. Porter, Evolution of Asian monsoons and phased uplift of the Himalaya–Tibetan plateau since Late Miocene times, Nature 411 (2001) 62–66.
[16] R. Hall, The plate tectonics of Cenozoic SE Asia and the distribution of land and sea, in: R. Hall, J.D. Holloway (Eds.), Biogeography and Geological Evolution of SE Asia, Backhuys, Leiden, 1998, pp. 99–131.
[17] R. Hall, Cenozoic geological and plate tectonic evolution of SE Asia and the SW Pacific: computer-based reconstructions, model and animations, J. Asian Earth Sci. 20 (2002) 353–431.
[18] P. Wang, W.L. Prell, P. Blum et al., Proc. ODP Init. Rep. 184 (2000) 1–77.
[19] P. Clift, J.I. Lee, M.K. Clark, J. Blusztajn, Erosional response of South China to arc rifting and monsoonal strengthening: a record from the South China Sea, Mar. Geol. 184 (2002) 207–226.
[20] R.J. Wang, D.Y. Fang, L. Shao, M.H. Chen, P.F. Xia, J.Y. Qi, Oligocene biogenic siliceous deposits on the slope of the northern South China Sea, Sci. China Ser. D 44 (2001) 912–918.
[21] R. Freydier, A. Michard, G. De Lange, J. Thomson, Nd isotopic compositions of Eastern Mediterranean sediments: tracers of the Nile influence during sapropel S1 formation?, Mar. Geol. 177 (2001) 45–62.
[22] X.H. Li, Y. Liu, X. Tu, G. Hu, W. Zeng, Precise determination of chemical compositions in silicate rocks using ICP-AES and ICP-MS: a comparative study of sample digestion techniques of alkali fusion and acid dissolution (in Chinese with English abstract), Geochimica 31 (2002) 289–294.
[23] X. Liang, G. Wei, X.H. Li, Y. Liu, Precise measurement of $^{143}Nd/^{144}Nd$ and Sm/Nd ratios using multiple-collectors inductively coupled plasma-mass spectrometer (MC-ICPMS) (in Chinese with English abstract), Geochimica 32 (2003) 91–96.
[24] D. Vance, M. Thirlwall, An assessment of mass discrimination in MC-ICPMS using Nd isotopes, Chem. Geol. 185 (2002) 227–240.
[25] T. Tanaka et al., JNdi-1: a neodymium isotopic reference in consistency with LaJolla neodymium, Chem. Geol. 168 (2000) 279–281.
[26] P.W. Fralick, B.I. Kronberg, Geochemical discrimination

of clastic sedimentary rock source, Sediment. Geol. 113 (1997) 111–124.
[27] H.W. Nesbitt, G. Markovice, R. Price, Chemical processes affecting alkalis and alkaline earths during continental weathering, Geochim. Cosmochim. Acta 44 (1980) 1659–1666.
[28] H.W. Nesbitt, G. Markovice, Weathering of granodioritic crust, long-term storage of elements in weathering profiles, and petrogenesis of siliciclastic sediments, Geochim. Cosmochim. Acta 61 (1997) 1653–1670.
[29] B.K. Nelson, D.J. DePaolo, Application of Sm–Nd and Rb–Sr isotopic systematics to studies of provenance and basin analysis, J. Sediment. Petrol. 58 (1988) 348–357.
[30] S.C. Cande, D.V. Kent, Revised calibration of the geomagnetic polarity timescale for the Late Cretaceous and Cenozoic, J. Geophys. Res. 100 (1995) 6093–6095.
[31] T.M. Harrison, P. Copeland, W.S.F. Kidd, A. Yin, Raising Tibet, Science 255 (1992) 1663–1670.
[32] M.E. Raymo, W.F. Ruddiman, Tectonic forcing of the late Cenozoic climate, Nature 359 (1992) 117–122.
[33] H. Zheng, C.M. Powell, Z. An, J. Zhou, G. Dong, Pliocene uplift of the northern Tibetan Plateau, Geology 28 (2000) 715–718.
[34] G. Ramstein, F. Fluteau, J. Besse, S. Joussaume, Effect of orogeny, plate motion and land-sea distribution on Eurasian climate change over the past 30 million years, Nature 386 (1997) 788–795.
[35] S.L. Goldstein, R.K. O'Nions, Nd and Sr isotopic relationships in pelagic clays and ferromanganese deposits, Nature 292 (1981) 324–327.
[36] S.L. Goldstein, R.K. O'Nions, P.J. Hamilton, A Sm–Nd isotopic study of atmospheric dusts and particulates from river systems, Earth Planet. Sci. Lett. 70 (1984) 221–236.
[37] J.F. Chen, B.M. Jahn, Crustal evolution of southeastern China: evidence from Sr, Nd and Pb isotopic compositions of granitoids and sedimentary rocks, Tectonophysics 284 (1998) 101–133.
[38] S.J. Goldstein, S.B. Jacobsen, Nd and Sr isotopic systematics of river water suspended material: implication for crustal evolution, Earth Planet. Sci. Lett. 87 (1988) 249–265.
[39] C.-H. Chen, B.M. Jahn, T. Lee, C.-H. Chen, J. Cornichet, Sm–Nd isotopic geochemistry of sediments from Taiwan and implications for the tectonic evolution of southeast China, Chem. Geol. 88 (1990) 317–332.
[40] T.C. Liew, M.T. McCulloch, Genesis of granitoid batholiths of peninsular Malaysia and implications for models of crustal evolution – evidence from a Nd–Sr isotopic and U–Pb zircon study, Geochim. Cosmochim. Acta 49 (1985) 587–600.
[41] C.Y. Lan, S.L. Chung, J.J.S. Shen, C.H. Lo, P.L. Wang, T.T. Hoa, H.H. Thanh, S.A. Mertzman, Geochemical and Sr–Nd isotopic characteristics of granitic rocks from northern Vietnam, J. Asian Earth Sci. 18 (2000) 267–280.
[42] R. Soeria-Atmadja, D. Noeradi, B. Priadi, Cenozoic magmatism in Kalimantan and its related geodynamic evolution, J. Asian Earth Sci. 17 (1999) 25–45.
[43] R. Rundick, D.M. Fountain, Nature and composition of the continental crust: a lower crustal perspective, Rev. Geophys. 33 (1995) 267–309.
[44] L. Shao, X.H. Li, G. Wei, Y. Liu, D. Fang, Provenance of a prominent sediment drift on the northern slope of the South China Sea, Sci. China Ser. D 44 (2001) 919–925.
[45] J. Wu, Evaluation and models of Cenozoic sedimentation in the South China Sea, Tectonophysics 235 (1994) 77–98.
[46] H.-S. Yu, The pearl River Mouth Basin: A rift basin and its geodynamic relationship with the southeastern Eurasian margin, Tectonophysics 183 (1990) 177–186.
[47] B.U. Haq, J. Hardenbol, P.R. Vail, Chronology of fluctuating sea levels since the Triassic, Science 235 (1987) 1156–1167.
[48] W. Huang, P.X. Wang, A quantitative approach to deep-water sedimentation in the South China Sea: Changes since the last glaciation, Sci. China Ser. D 41 (1998) 195–201.
[49] S.L. Chung, T.Y. Lee, C.H. Lo, P.L. Wang, C.Y. Chen, N.T. Yem, T. Huo, G. Wu, Intraplate extension prior to continental extrusion along the Ailao Shan–Red River shear zone, Geology 25 (1997) 311–314.
[50] S.L. Chung, C.H. Lo, T.Y. Lee, Y. Zhang, Y. Xie, X. Li, K.L. Wang, P.L. Wang, Diachronous uplift of the Tibetan plateau staring 40 Myr ago, Nature 394 (1998) 769–773.
[51] P.L. Wang, C.H. Lo, T.Y. Lee, S.L. Chung, C.Y. Lan, N.T. Yem, Thermochronological evidence for the movement of the Ailao Shan–Red River Shear Zone: A perspective from Vietnam, Geology 26 (1998) 887–890.
[52] U. Schärer, P. Tapponnier, R. Lacassin, P.H. Leloup, D. Zhong, S. Ji, Intraplate tectonics in Asia: A precise age for large-scale Miocene movement along the Ailao-Shan–Red River shear zone, China, Earth Planet. Sci. Lett. 97 (1990) 65–77.
[53] U. Schärer, L.-S. Zhang, P. Tapponnier, Duration of strike-slip movements in large shear zones: The Red River belt, China, Earth Planet. Sci. Lett. 126 (1994) 379–397.
[54] L.-S. Zhang, U. Schärer, Age and origin of magmatism along the Cenozoic Red River shear belt, China, Contrib. Mineral. Petrol. 134 (1999) 67–85.
[55] J.H. Wang, A. Yin, T.M. Harrison, M. Grove, Y.Q. Zhang, G.H. Xie, A tectonic model for Cenozoic igneous activities in the eastern Indo-Asian collision zone, Earth Planet. Sci. Lett. 188 (2001) 123–133.
[56] R. Lacassin, C. Hinthong, K. Siribhakdi, S. Chauviroj, A. Charoenravat, H. Maluski, P.H. Leloup, P. Tapponnier, Tertiary diachronic extrusion and deformation of western Indochina: structure and $^{40}Ar/^{39}Ar$ evidence from NW Thailand, J. Geophys. Res. 102 (1997) 10013–10037.